Ab-Initio Study of Hyperfine Structure of M7 (M=Li, Na, K, Cu and Ag) Clusters, Using All-Electron Mixed-Basis Method

著者	Bahramy Mohammad Saeed, Kawazoe Yoshiyuki
journal or publication title	Materials Transactions
volume	48
number	7
page range	1883-1885
year	2007
URL	http://hdl.handle.net/10097/52327

Materials Transactions, Vol. 48, No. 7 (2007) pp. 1883 to 1885

Ab-Initio Study of Hyperfine Structure of M_7 (M = Li, Na, K, Cu and Ag) Clusters, Using All-Electron Mixed-Basis Method

Mohammad Saeed Bahramy* and Yoshiyuki Kawazoe

Institute for Materials Research, Tohoku University, Sendai, 980-8577 Japan

Within density functional theory, the geometrical properties and the hyperfine structure of 7-atom clusters, $^{7}Li_7$, $^{23}Na_7$, $^{39}K_7$, $^{63}Cu_7$ and $^{107}Ag_7$ are investigated using the so-called all-electron mixed basis method. The calculations reveal that all the clusters have a pentagonal bipyramidal geometry with a D_{5h} symmetry in which an unpaired electron occupies an a_2'' state. It turns out that, the unpaired electron in all the clusters is mostly distributed on the axial sites with a minor contributions at the pentagonal ring sites. The calculated spin distributions and the isotropic hyperfine parameters are in excellent agreement with the corresponding experimental data.
[doi:10.2320/matertrans.N-MRA2007857]

(Received January 3, 2007; Accepted April 17, 2007; Published June 13, 2007)

Keywords: *hyperfine parameters, spin distribution, metal clusters, all-electron mixed-basis method*

1. Introduction

The intense interest and research activity in metal clusters, both naked and ligated, continues unabated.[1–3] These intermediate species are "neither fish nor fowl" and have interesting geometries and electronic structures with a rich chemistry.[4,5] They can be good models for the active centers in catalysts and are the nuclei for phase changes and for the silver halide photographic process.[6] Recent molecular calculations also suggests that metal clusters are unique in having an appreciable aggregation of electron density in the bonds between the metal nuclei.[7]

Experimentally, much of our knowledge on the geometrical and electronic structure properties of metal clusters have been obtained through the analysis of their hyperfine structures (HFS's), as probed by spectroscopic techniques such as electron spin resonance (ESR)[8] or nuclear magnetic resonance (NMR).[9] In the particular case of M_7 clusters, where M is either an alkali metal (Li, Na, or K) or a noble metal (Cu or Ag), the ESR studies reveal a striking similarity in the geometric and electronic structures of these clusters.[10–13] On the basis of these studies, all the M_7 clusters have a pentagonal bipyramidal geometry with a D_{5h} symmetry. Also, the ground state wavefunctions of the clusters is expected to be most likely $^2A_2''$ with an unpaired electron occupying an a_2'' state. Furthermore, in all the M_7 clusters, the unpaired electron is substantially more localized on the two magnetically equivalent axial atoms than the rest of five magnetically equivalent pentagonal ring atoms.

Theoretically, the previous first-principles calculations have also indicated that the most stable configuration of the considered M_7 clusters have a pentagonal bipyramidal geometry with a D_{5h} symmetry.[14–16] In this paper, we present the result of the density functional theory (DFT) calculations of the magnetic hyperfine parameters of these M_7 clusters using the so-called all-electron mixed-basis (AEMB) method.[17] The calculated spin distribution and magnetic hyperfine parameters (HFP's) fully support the ESR identification of a cluster composed of seven M atoms with a pentagonal bipyramid structure. Additionally, our calculations indicate that the single unpaired electron in all the clusters is substantially localized on the two axial M atoms.

2. Computational Details

The AEMB wavefunctions are constructed by employing both confined atomic orbitals (AO's) and plane waves (PW's) as basis function.[17] The AO's are utilized to represent the charge and spin density at, and in the vicinity of, the atomic nuclei, of particular importance for calculating hyperfine parameters, whereas the PW part of wavefunctions is computationally expedient and are only needed to compensate the deviation of the actual eaigenstates from those of the atomic configuration. In the previous work,[17] we showed that a cutoff energy of about 200 eV for the PW expansion of wavefunctions is of adequate accuracy to serve for calculating the HFP's of clusters.

Once the spin-polarized AEMB wavefunctions $\Psi_{\lambda\sigma}$ are constructed for all energy levels λ in both spin channels σ ($\uparrow$ and $\downarrow$), the spin density $\rho^s(\mathbf{r})$ is calculated by $\rho^s(\mathbf{r}) = \rho_\uparrow(\mathbf{r}) - \rho_\downarrow(\mathbf{r})$, where $\rho_\sigma(\mathbf{r})$ is the electron charge density with spin σ, defined as $\rho_\sigma(\mathbf{r}) = \sum_\lambda \langle\Psi_{\lambda\sigma}|\Psi_{\lambda\sigma}\rangle$. Subsequently, the isotropic HFP $A_{iso}(I)$, known also as Fermi contact parameter, is computed with,

$$A_{iso}(I) = \frac{2}{3}\mu_0 g_e \mu_e g_I \mu_I \rho_s(\mathbf{R}_I), \tag{1}$$

where, $\mathbf{R}_I$ is the position of nucleus I, μ_0 is the permeability of vacuum ($4\pi \times 10^{-7}\,\mathrm{T^2\,m^3\,J^{-1}}$), g_e is the electron g factor, μ_e is the Bohr magneton, g_I and μ_I are the gyromagnetic ratio and the magnetic moment of the nucleus. Throughout this work, g_I and μ_I values are taken from Ref. 18).

The DFT calculations have been carried out within local spin density approximation (LSDA).[19] Accurate forces were obtained with a potential cutoff energy of about 1000 eV for all clusters. To minimize the overlap between the wavefunctions of the clusters in the neighbor cells, we consider a cubic supercell with a side of 16 Å for each of the structures. The first Brillouin zone is sampled at the Γ point only. The clusters were structurally relaxed until the magnitude of the force is less than 0.001 eV/Å on every atom.

*Corresponding author, E-mail: saeed@imr.edu

Table 1 Optimal geometries (in Å) of the M_7 alkali and noble metal clusters.

Cluster (M_7)	d(M(2)—M(5))	d(M(5)—M(5))
$^{7}Li_7$	2.984	2.927
$^{23}Na_7$	3.676	3.395
$^{39}K_7$	4.801	4.209
$^{63}Cu_7$	2.475	2.392
$^{107}Ag_7$	2.667	2.622

3. Results and Discussion

Table 1 shows the optimized distances d(M(2)—M(5)) and d(M(5)—M(5)) of all M_7 clusters, where M(2) and M(5) indicate the two equivalent axial and the five equivalent pentagonal ring atoms, respectively. The similarities among the clusters are evident. The table indicates that, d(M(2)—M(5)) is larger than d(M(5)—M(5)) for all the clusters. Furthermore, our calculations confirm the experimentally observed $^2A_2''$ state with an unpaired electron occupying an a_2'' molecular orbital, as the ground state wavefunction of these clusters. The singly occupied a_2'' orbital exhibits a large s-character at the apical atoms and quite significant p-character at the pentagonal ring atoms.

Table 2 summarizes the spin distributions (ρ) and the corresponding isotropic HFP's for the $^2A_2''$ ground state of the M_7 clusters as computed using AEMB method and as obtained from the ESR experiments. The Table indicates a good agreement between the results of AEMB calculations of isotropic HFP's clusters with the corresponding experimental data for all the M_7 clusters. This implies that, the experimentally predicted pentagonal bipyramidal structure with D_{5h} symmetry is correctly the ground state structure of all these septamer clusters. It is to be noted that, the sign of the spin distributions and the isotropic HFP's on the ring nuclei can not be directly identified through the ESR measurement, because of their smallness. However, it turns out from AEMB calculations that the signs of $\rho(5)$ and $A_{iso}(5)$ in all M_7 are positive and negative, respectively (see Table 2). The only exception is the $A_{iso}(5)$ of $^{107}Ag_7$ which is positive. The reason will be discussed later.

A more detailed analysis of the spin distributions reveals that $j = 1/2$ states dominate substantially the spin densities around both the axial and ring nuclie of all the M_7 clusters, whereas the contribution of $j = 3/2$ and $5/2$ states are negligibly less pronounced. It is well known that,[17,20] the spin distributions arising from $j = 1/2$ are spherically symmetric, and its contributions to the hyperfine interactions are isotropic, while the spin distributions arising from $j = 3/2$ and $5/2$ states give rise to anisotropic magnetic interactions since these are nonspherical contributions. As a consequence, the anisotropy of hyperfine couplings is expected to be negligible.

As indicated in Table 2, the spin population on the two equivalent apical nuclei is significantly larger than that on the remaining five equivalent pentagonal nuclei. This trend of distribution is qualitatively similar among all the clusters. The existing difference between the experimental and theoretical values of both $\rho(2)$ and $\rho(5)$ is due to the fact that, $\rho(2)$ and $\rho(5)$ are experimentally defined as the ratio of the $A_{iso}(2)$ and $A_{iso}(5)$ of the considered apical and basal atoms of the M_7 clusters to that of the corresponding free M atoms, respectively, by taking into account only the s-character and neglecting p- and d-contributions. As a result, the summation over all the spin distributions, $\rho_{tot} = (2\rho(2) + 5\rho(5))$ becomes less than one, as shown in Table 2. In the AEMB calculations, however, the contributions of all orbitals are included in the evaluation of $\rho(2)$ and $\rho(5)$ so that ρ_{tot} is always equal to one, as it should be.

One can notice from Table 2 that in all the M_7 clusters, $A_{iso}(2)$ is substantially larger than $A_{iso}(5)$. This is because of two reasons. The first reason is that, the spin distribution is more localized on the apical sites than the basal sites ($\rho(2) \gg \rho(5)$). Thus, the hyperfine coupling is expected to be larger on the axial nuclei than that on the pentagonal ones. The second and more important reason is that, as mentioned above, the localized spin densities on the apical sites are significantly dominated by the s-like electrons whereas the p- and/or d-orbitals contribute substantially to the spin density on the pentagonal sites. Since, the isotropic HFP is proportional to the spin density at the nucleus point, arising from s-electrons ($j = 1/2$), it is thus expected that the $A_{iso}(2)$ values become substantially larger than the $A_{iso}(5)$ values.

Interestingly, the sign of the calculated $A_{iso}(5)$ parameters in all the clusters are opposite to that of the corresponding $\rho(5)$ values, except for $^{107}Ag_7$ in which both $A_{iso}(5)$ and $\rho(5)$ are positive. Since the g_I is negative for ^{107}Ag and positive for the rest of M atoms, this implies that the net contribution of spin densities at the position of pentagonal nuclei, $\rho_s(\mathbf{R}_5)$ in eq. (1), must be negative. In other words, the effective magnetic moment at the nuclei of the pentagonal ring atoms is opposite to that of the unpaired a_2'' electron. This is due to the spin polarization of the paired core and valence orbitals, induced by the unpaired electron through its exchange interaction with the inner paired electrons in the same spin channel.[17] The dominant p- and/or d-characters of spin

Table 2 Comparison of the spin distributions and the isotropic hyperfine parameters (in MHz) in the pentagonal bipyramidal-type M_7 clusters.

Cluster (M_7)	AEMB method				Experiment[a]			
	$\rho(2)$	$\rho(5)$	$A_{iso}(2)$	$A_{iso}(5)$	$\rho(2)$	$\rho(5)$	$A_{iso}(2)$	$A_{iso}(5)$
$^{7}Li_7$	0.301	0.080	100.1	−6.0	0.254	±0.015	101.9	±6.1
$^{23}Na_7$	0.347	0.061	335.3	−17.5	0.370	±0.021	327.6	±18.2
$^{39}K_7$	0.350	0.060	89.7	−2.3	0.371	±0.022	85.5	±5.0
$^{63}Cu_7$	0.315	0.074	1750.4	−51.3	0.291	±0.009	1747	±54.0
$^{107}Ag_7$	0.396	0.042	−613.9	11.5	0.324	±0.001	685.0	±25.4

[a]Experimental data from Ref. 10) ($^{7}Li_7$), Ref. 11) ($^{23}Na_7$ and $^{39}K_7$), Ref. 12) ($^{63}Cu_7$), and Ref. 13) ($^{107}Ag_7$).

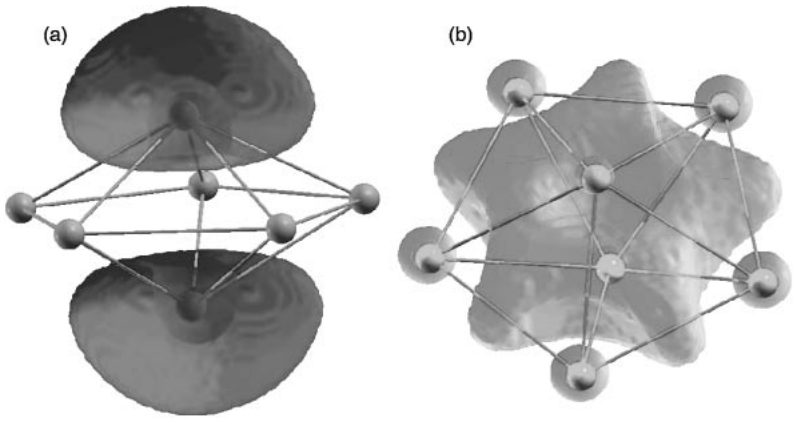

Fig. 1 Spin densities arising from (a) the unpaired a_2'' state and (b) the spin polarized inner core and valence levels in $^{23}Na_7$ cluster. The iso-surfaces are plotted for (a) $\rho_s = 0.005\,\mathrm{eV/\AA^3}$ and (b) $\rho_s = -0.001\,\mathrm{eV/\AA^3}$.

densities at the pentagonal sites can not directly contribute to the $A_{iso}(5)$ parameters. However, they can slightly spin polarize the core and valence *s*-electrons so that, the net contribution of spin density at the site of pentagonal nuclei becomes non-zero. Such a contribution is always negative for atoms with *p* and/or *d*-like singly occupied molecular orbitals (SOMO).[17,21] Accordingly, the $A_{iso}(5)$ values of the M_7 clusters turn out to be negative. The above discussion leads to this conclusion that the proper description of hyperfine parameters of metallic clusters (and even other species) needs the inclusion of the core spin polarization effects. It is worth mentioning that, the mentioned negative contribution of core levels to the hyperfine field was long time ago pointed out and discussed by Jena *et al.*[22]

In order to get a visual picture of the spin distributions on different sites, the spin densities arising from SOMO and the spin polarized inner orbitals are plotted in Figs. 1(a) and 1(b) for Na_7. The former clearly indicates that the unpaired electron reside substantially on the apical atoms. On the other hand, Figure 1(b) reveals that the spin density arising from the spin polarized core and valence orbitals is significantly distributed on the plane of the pentagonal ring with only minor contributions at the apical sites.

4. Conclusions

In summary, It was shown that the AEMB results of the spin distributions and the isotropic hyperfine parameters of 7-atom clusters $^7Li_7$, $^{23}Na_7$, $^{39}K_7$, $^{63}Cu_7$ and $^{107}Ag_7$ agree well with the ESR measurements. The consistency between the clauclated and observed data led to this conclusion that these clusters have a pentagonal bipyramid structure with a D_{5h} symmetry. It turned out that the majority of the unpaired *s*-electrons ($j = 1/2$) reside on the two equivalent apical sites of the clusters, and a small remaining fraction is equally distributed over the five equivalent pentagonal ring nuclei.

Acknowledgment

The authors gratefully would like to acknowledge the center for computational materials science (CCMS) at the institute for materials Research (IMR) for the allocations on the Hitachi SR8000 supercomputer system. MSB would like to thank Dr. M. Itoh for many instructive discussions and helpful information, regarding the hyperfine structure of Cu_7.

REFERENCES

1) M. Moskovits and L. Andrews (Ed.): *Chemistry and physics of matrix isolated species*, (North-Holland, Amsterdam, 1989).
2) J. A. Howard and B. Mile: Accounts Chem. Res. **20** (1987) 173–179.
3) W. A. de Heer: Rev. Mod. Phys. **65** (1993) 611–675.
4) C. A. Hampson, M. Histed, J. A. Howard, H. Morris and B. Mile: Faraday Discussions **92** (1991) 129–145.
5) O. Echt and E. Recknayel (Ed.): *Small particles and inorganic clusters*, (Springer, Berlin, 1990).
6) E. Moisar: Photograph. Sci. Eng. **26** (1982) 124-124.
7) W. L. Cao, C. Gatti, P. J. Macdougall and F. W. Bader: Chem. Phys. Lett. **141** (1987) 380–385.
8) A. Abragam and B. Bleaney: *Electronic Paramagnetic Resonance of Transition Ions* (Clearendon Press, Oxford, 1970).
9) I. Bertini, C. Luchinat and G. Parigi: *Solution NMR of paramagnetic molecules* (Elsevier, Amsterdam, 2001).
10) D. A. Garland and D. M. Lindsay: J. Chem. Phys. **80** (1984) 4761–4766.
11) G. A. Thompson, F. Tischler and D. M. Lindsay: J. Chem. Phys. **78** (1983) 5946–5953.
12) R. J. van Zee and W. Weltner, Jr.: J. Chem. Phys. **92** (1990) 6976–6977.
13) S. B. H. bach, D. A. Garland, R. J. van Zee and W. Weltner, Jr.: J. Chem. Phys. **87** (1987) 869–872.
14) P. Fantucci, J. Koutecký and G. Pacchioni: J. Chem. Phys. **80** (1983) 325–328.
15) R. Arratia-Pérez, L. Alvarez-Thon and P. Fuentealba: Chem. Phys. Lett. **397** (2004) 408–411.
16) R. Arratia-Pérez, L. Hernández-Acevedo and L. Alvarez-Thon: J. Chem. Phys. **108** (1998) 5795–5798.
17) M. S. Bahramy, M. H. F. Sluiter and Y. Kawazoe: Phys. Rev. B **73** (2006) 045111; 1–21.
18) D. R. Lide: *Handbook of Chemistry and Physics* (CRC press, Boca Raton, 2004), 85th edition, pp. **9**-93-**9**-95.
19) J. P. Perdew and A. Zunger: Phys. Rev. B **23** (1981) 5048–5079.
20) J. A. Weil, J. R. Bolton and J. E. Wertz: *Electron Paramagnetic Resonance: Elementary Theory and Practical Applications* (Wiley, New York, 1994).
21) M. L. Munzarová, P. Kubáček and M. Kaupp: J. Am. Chem. Soc. **122** (2000) 11900–11913.
22) P. Jena, S. D. Mahanti and T. P. Das: Phys. Rev. Lett. **20** (1968) 544–546.